Sustainable Cities and Society 97 (2023) 104727

Contents lists available at ScienceDirect

Sustainable Cities and Society

journal homepage: www.elsevier.com/locate/scs

The contribution of metropolitan areas to decarbonize the residential stock in Mediterranean cities: A GIS-based assessment of rooftop PV potential in Valencia, Spain

Ivan Cuesta-Fernández, Carlos Vargas-Salgado *, David Alfonso-Solar, Tomás Gómez-Navarro

Institute for Energy Engineering, Universitat Politècnica de València, Camí de Vera s/n, Valencia, Spain

ARTICLE INFO

Keywords:
Self-sufficiency
Mediterranean cities
Solar energy
PV potential
Renewable energy

ABSTRACT

Hundreds of cities worldwide have committed to decarbonizing or becoming carbon neutral by 2030, 2050, or even sooner. The challenge is particularly acute for the dense, compact cities of the European Mediterranean basin. To maximize their energy self-sufficiency, Mediterranean cities seek to scale up PV production within their boundaries and supply themselves from ground-mounted plants in their surroundings. This paper provides an alternative approach based on the energy exchange between cities and their metropolitan areas. The potential of the approach is demonstrated by the results attained under a less favorable (conservative) scenario: supplying the electricity demand of the residential stock exclusively with rooftop PV. Drawing on a combination of spatial analysis (based on cadastral and statistical data) and energy simulation (with HOMER), the approach is applied to Valencia, Spain's city and its metropolitan area. Results show that rooftop PV may increase the PV coverage rate from 61% (Valencia and its first metropolitan ring) to 79.2% (whole metropolitan area) – or about 30% in relative terms. This may encourage Mediterranean cities to develop innovative urban-metropolitan energy exchange models, hopefully under the criteria of spatial justice.

1. Introduction

Hundreds of cities worldwide have committed to decarbonize or become carbon neutral by 2050, 2030, or even sooner, under the leadership of multiple initiatives such as the Covenant of Mayors or the platform of global cities C40 incl. Local authorities thus wake up to the Jano-faced nature of cities: the territorial unit that most contributes to climate change and the hub for the technical and social innovations that may nurture the required solutions (Mi et al., 2019, Pincetl, 2017, Droege, 2018). The problem is particularly salient for the dense, compact cities of the European Mediterranean basin. Given their population density and the spatial density of energy consumption, decarbonizing compact Mediterranean cities is the very definition of a 'wicked problem' in the trajectory towards a net-zero European Union (Cramer et al., 2018). To minimize land use and related adverse impacts beyond their boundaries, especially in rural areas, strategies to make Mediterranean cities climate-neutral often give a prominent role to the large-scale deployment of rooftop photovoltaics (PV) (Ruiz-Campillo, Gil, and García Fernández, 2022), (Burger and Luke, 2017).

Most often, maximizing rooftop PV generation in cities almost automatically translates into maximizing two indicators: installed capacity (PW power, often measured in MW) and PV coverage rate (or the share of PV generation compared to the energy/electricity demand of the city) (Fakhraian et al., 2021). It is hardly surprising, then, that the bulk of the efforts of energy researchers and urban planners has gravitated toward quantifying the maximum potential for PV generation in (Mediterranean) cities – and, eventually, the maximum coverage rate (Natanian and Auer, 2018), (Hosseini, 2019). Several studies have estimated the PV potential fraction of residential electricity consumption in the range of 20-40%, with some outliers in the range of 60-70% (for a list of case studies, see (Fakhraian et al., 2021)). This alone speaks of the need to approach the problem from new angles, such as the exchange of solar energy between cities and their metropolitan areas suggested here, which offer a suitable complement to already tested solutions, such as renewable-based mini- and micro-grids (Korkas, Baldi, Michailidis, and Kosmatopoulos, 2015, Korkas, Baldi, and Kosmatopoulos, 2018, Korkas, Baldi, Michailidis, and Kosmatopoulos, 2016).

Unfortunately, studies that quantify the contribution of metropolitan areas to the PV potential of their cities are virtually non-existent. But a growing number of studies of the PV potential of Mediterranean cities

* Corresponding author.
E-mail address: carvarsa@upvnet.upv.es (C. Vargas-Salgado).

https://doi.org/10.1016/j.scs.2023.104727
Received 5 October 2022; Received in revised form 11 June 2023; Accepted 11 June 2023
Available online 13 June 2023

have established the extent of the challenge of maximizing PV self-generation within the boundaries of dense, compact cities (Natanian and Auer, 2018), (Vulkan, Kloog, Dorman, and Erell, 2018). Elsewhere, large-scale studies have also shown a sizeable potential for urban rooftop PV. For example, in 2016, NREL estimated that rooftops in California could generate an equivalent to 74% of the electricity sold by utilities in 2013, with small rooftops hosting about 65% of the overall rooftop potential (Gagnon et al., 2016). Methods to assess the PV potential of urban areas can be classified according to two main approaches: GIS-based and non-GIS-based statistical methods. GIS-based methods draw on cartographic data, e.g. cadastral data, often also building upon LiDAR and occasionally machine learning, to calculate the available rooftop surface in great detail (Gassar and Cha, 2021, Song et al., 2018, Ren, Xu, Ma, and Sun, 2022, Bódis et al., 2019). These methods are characterized by the need to reach a compromise between accuracy and computation time (Gassar and Cha, 2021), (Freitas, Catita, Redweik, and Brito, 2015, Margolis et al., 2017, Ramirez Camargo and Stoeglehner, 2018, Groppi, de Santoli, Cumo, and Astiaso Garcia, 2018, Choi, Suh, and Kim, 2019, Castellanos, Sunter, and Kammen, 2017). In Mediterranean cities, this approach was applied in Nador (Lambarki, Maanan, and Rhinane, 2020), Istanbul (Yildirim, Büyüksalih, and Şahin, 2021), and Turin (Bergamasco and Asinari, 2011), although most studies date from the eartly- to mid-2010s. More recently, this approach has been also applied to Valencia (the case study in this work) (Gómez-Navarro, Brazzini, Alfonso-Solar, and Vargas-Salgado, 2021). Non-GIS methods often estimate available surfaces by extrapolating from a sample of representative building typologies (Horváth, Kassai-Szoó, and Csoknyai, 2016), (Fakhraian et al., 2021). Applications in the Mediterranean region include Barcelona (Izquierdo, Rodrigues, and Fueyo, 2008), (Torres-Rivas, Palumbo, Jiménez, and Boer, 2022) or Beirut (Eslami, Najem, Ghanem, and Ahmad, 2021). This method has also been tested in Valencia in several studies (Vargas-Salgado, Aparisi-Cerdá, Alfonso-Solar, and Gómez-Navarro, 2022, Fuster-Palop et al., 2021, Aparisi-Cerdá, Ribó-Pérez, Cuesta-Fernandez, and Gómez-Navarro, 2022). However, and to the best of our knowledge, to date no study has attempted to explore, let alone quantify, the potential of urban-metropolitan exchanges for the self-sufficiency of compact, dense Mediterranean cities.

Against this background, this paper seeks to establish the potential that large-scale deployment of rooftop PV in metropolitan areas may offer to the energy self-sufficiency of dense, compact Mediterranean cities. A literature review has identified a dearth of studies evaluating such potential in European cities. Concerning the contribution of metropolitan areas to the energy self-sufficiency of their capital cities, Mediterranean metropolitan areas offer several advantages. They are often less dense and compact than their cities (Munoz, 2003), thus providing a better generation-to-available-surface ratio. Also, in Mediterranean metropolitan areas, consumption between residential, commercial, and industrial customers is more balanced than in their cities (dominated by the residential sector). This is singularly relevant for photovoltaic technologies, in which generation is only available during daylight hours. Lesser weights of residential patterns, which tend to concentrate their consumption in the very early and late hours of the day, often outside daylight hours, facilitate more efficient photovoltaic systems (Natanian, Aleksandrowicz, and Auer, 2019, Vartholomaios, 2017, Morganti, Salvati, Coch, and Cecere, 2017).

In this study, the analysis is restricted to satisfying the electric demand of the residential stock. Increasing the coverage rate of the residential stock with rooftop-mounted PV is arguably one of the least favorable and most demanding scenarios. Therefore, a significant increase in the coverage rate under this scenario provides a promising starting point for a future, more complete assessment of the potential of urban-metropolitan exchanges. Besides, the approach pursued in this article is premised on the translation to city-metropolitan geographies of existing models that establish virtual energy exchanges between rooftop-constrained urban households and PV generation in rural utility-scale, ground-mounted solar plants (Capellán-Pérez, Campos-Celador, and Terés-Zubiaga, 2018), (Moura and Brito, 2019). The outline and particular characteristics of such city-metropolitan exchange models falls beyond the scope of this article.

Against this background, this article assesses the untapped potential of innovative, urban-metropolitan virtual energy exchanges to increase the rate of renewable coverage in the city of Valencia. To do so, it estimates, with the help of GIS-based methods, the photovoltaic potential of rooftops in the residential stock of the metropolitan area. The article proceeds as follows. The following section briefly presents the case study and introduces a methodology to estimate the PV potential in compact, dense metropolitan areas. The metropolitan area of Valencia, Spain, is summarized according to the singularities of the territorial units (first and second metropolitan ring) under analysis. The third section presents the main results obtained with QGIS and HOMER. Two scenarios are compared to assess the metropolitan area's potential contribution to PV generation. Scenario 1 includes the city of Valencia and the first ring of its metropolitan area. Scenario 2 aggregates the city of Valencia and the first and second metropolitan rings. Results are presented in terms of three key variables: potential PV installed capacity, electricity generation, and PV coverage rate. The article concludes by discussing the results and the policy implications of this work, as well as potential avenues for further research(Fig. 1).

2. Methods

This section presents the method employed to quantify the PV coverage rate of the metropolitan residential stock of Valencia as satisfied with rooftop PV. The sequence is as follows: first, the method estimates the exploitable area in the city's rooftops and the metropolitan area. To do so efficiently, the method samples a significant portion of the metropolitan municipalities (see Table 1). It also filters out potentially misleading spatial polygons in the sample's cadastral database of the municipalities (see Figs. 2 and 3). This analysis produces a conservative estimation of the exploitable rooftop area in Valencia and its metropolitan area (see Tables 6-8. Second, the method simulates PV production with the assistance of the HOMER software (see Fig. 4). PV production in the first and second metropolitan rings of Valencia, combined with an estimation of energy demand (see Fig. 5 and Table 2), allows estimating the PV coverage rate (see Tables 9 and 10). The subsections below explain the method in detail.

2.1. Sample of municipalities in the metropolitan area

The metropolitan area of Valencia is composed of 57 municipalities – 41 in the so-called first ring and 15 in the second ring. To diminish computing requirements for the GIS analysis, minimizing the number of municipalities under study is convenient. The municipalities are thus sampled as follows: first, all municipalities in the 1st metropolitan ring are ranked by descending population; second, municipalities are added to the sample in descending order until at least 70% of the metropolitan population is included. This sampling threshold of 70% is derived from the Pareto principle, which is widely accepted in economics and engineering. The principle suggests that roughly 20% of causes contribute to 80% of outcomes or effects. By targeting 70% of the population, we wish to capture a significant proportion of the more influential municipalities. Thus, upon analyzing the first ring of the Valencia metropolitan area, it becomes evident that 6 municipalities, comprising 15% of the total, account for a significant 70.2% of the overall population. Therefore, we choose to restrict the GIS analysis to a sample of these 6 municipalities, expected to exert significant influence on the study's outcomes. For the 2nd ring, a higher variety of urban morphologies and building stock, is found. Again, a conservative approach recommends including the 15 municipalities of the 2nd ring. Overall, the localities sampled for GIS analysis in the 1st and 2nd rings account for 73.7% of the overall metropolitan population (see Table 1). It is important to note

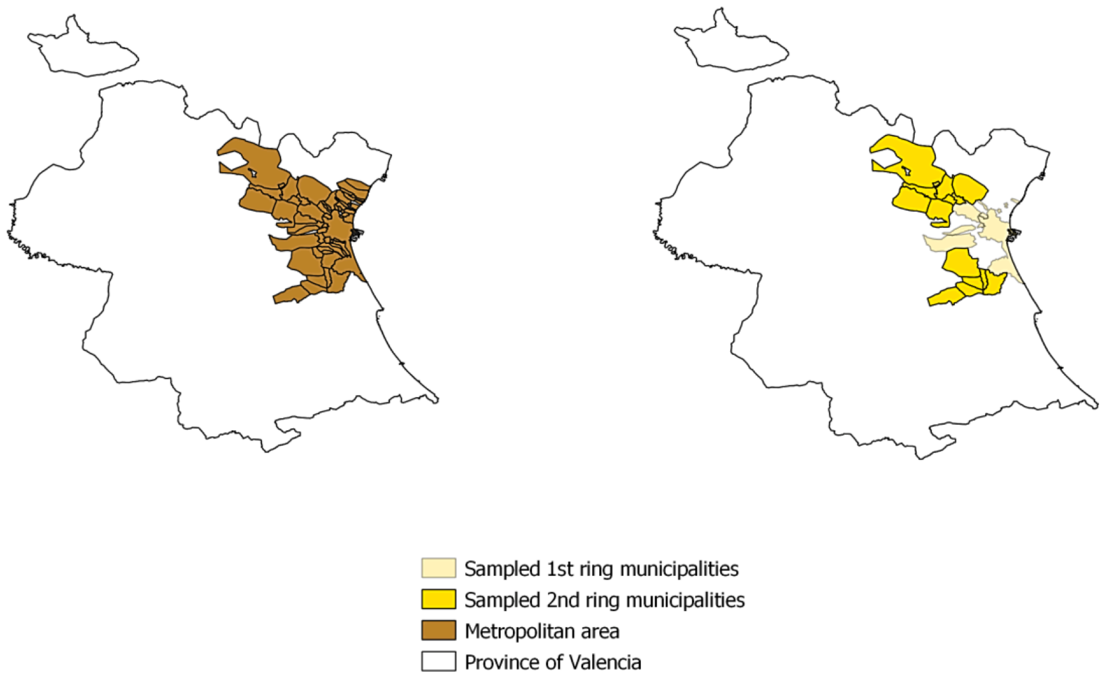

Fig. 1. Sampled municipalities in the metropolitan area of Valencia. Source: Own elaboration based on (Capellán-Pérez, Campos-Celador, and Terés-Zubiaga, 2018).

Table 1
Population by municipality (with Pareto-like analysis) in the first and second ring of the metropolitan area of Valencia. Source: Instituto Nacional de Estadística (Generalitat Valenciana), ('Instituto Nacional de Estadística. (National Statistics Institute) 2022).

	Municipality	Population (2021)	As a % of the metropolitan area
First ring			
1	Valencia	789,744	52.3%
2	Torrent	84,025	5.6%
3	Paterna	71,361	4.7%
4	Mislata	44,320	2.9%
5	Burjassot	38,712	2.6%
6	Aldaia	32,313	2.1%
7	Other (35 municipalities)	449,878	29.8%
	6 sampled municipalities	1,060,475	70.2%
	Total	1,510,353	100.0%
Second ring			
1	Alginet	13,057	6.6%
2	Almussafes	8,189	4.1%
3	Benaguasil	10,728	5.4%
4	Benifaió	12,119	6.1%
5	Benisanó	2,136	1.1%
6	Bétera	20,292	10.2%
7	Carlet	15,366	7.8%
8	L'Eliana	16,549	8.3%
9	Llíria	22,441	11.3%
10	Picassent	19,385	9.8%
11	Pobla de Vallbona	19,540	9.9%
12	Riba-roja	19,938	10.1%
13	San Antonio de Benagéber	5,330	2.7%
14	Sollana	4,889	2.5%
15	Vilamarxant	8,257	4.2%
	Total	198,216	100.0%

that by discarding 85% of the municipalities in the 1st ring, our sampling tends to underestimate the PV potential of the area.

Table 1 enumerates the municipalities included in the sample. The 1st ring includes Valencia, Torrent, Paterna, Mislata, Burjassot, and Aldaia. The 2nd ring includes Alginet, Almussafes, Benaguasil, Benifaió, Benisanó, Bétera, Carlet, L'Eliana, Llíria, Picassent, Pobla de Vallbona, Riba-roja, San Antonio de Benagéber, Sollana, and Vilamarxant.

It is important to bear in mind that by sampling municipalities, the PV potential of the metropolitan area is likely to be underestimated. This stems from the fact that the 1st and 2nd rings differ not only in population (see Table 1) but, crucially, in the nature of the building stock. Higher buildings are more common in the 1st ring than in the 2nd. Final results must therefore be evaluated with this caveat in mind.

2.2. Determination of the exploitable stock of residential buildings

A thorough analysis of the Spanish official cadastral database reveals a number of shortcomings. Spatial polygons of one height are especially problematic. Thus, it is not uncommon that large polygons with commercial use are catalogued as residential. Also, spatial polygons of less than 20 m^2 may correspond to areas unsuitable for PV production, such as elevator machinery cabins, courtyards, skylights, or simply fractions of the building. To address these two problems, the method filters out buildings of less than two heights, and small spatial polygons of less than 20 m^2, notably commercial centers, in the cadastral database. The robustness of the filter was contrasted via a manual analysis of a random sample of rooftops across one-fourth of the municipalities. No significant errors were found. Again, it is essential to remember that filtering out by surface contributes to underestimating the PV potential. For the whole metropolitan area, the combined effect of both filters discards 8.36 % of the estimated rooftop area. The impact of the height filter may be more relevant when calculating the PV potential of specific localities, especially in the 2nd ring. Filtering outbuildings of one height in the 2nd ring discards about one-third of the overall rooftop surface.

Fig. 2 and Fig. 3 illustrate the effect of the 20 m^2 filter in Valencia and San Antonio de Benagéber, respectively the most and least populated municipalities in the sample.

2.3. Estimation of residential rooftop area and actual area for exploitation

With the help of QGIS software, cadastral data has been processed for each municipality in the sample to estimate the surface available in

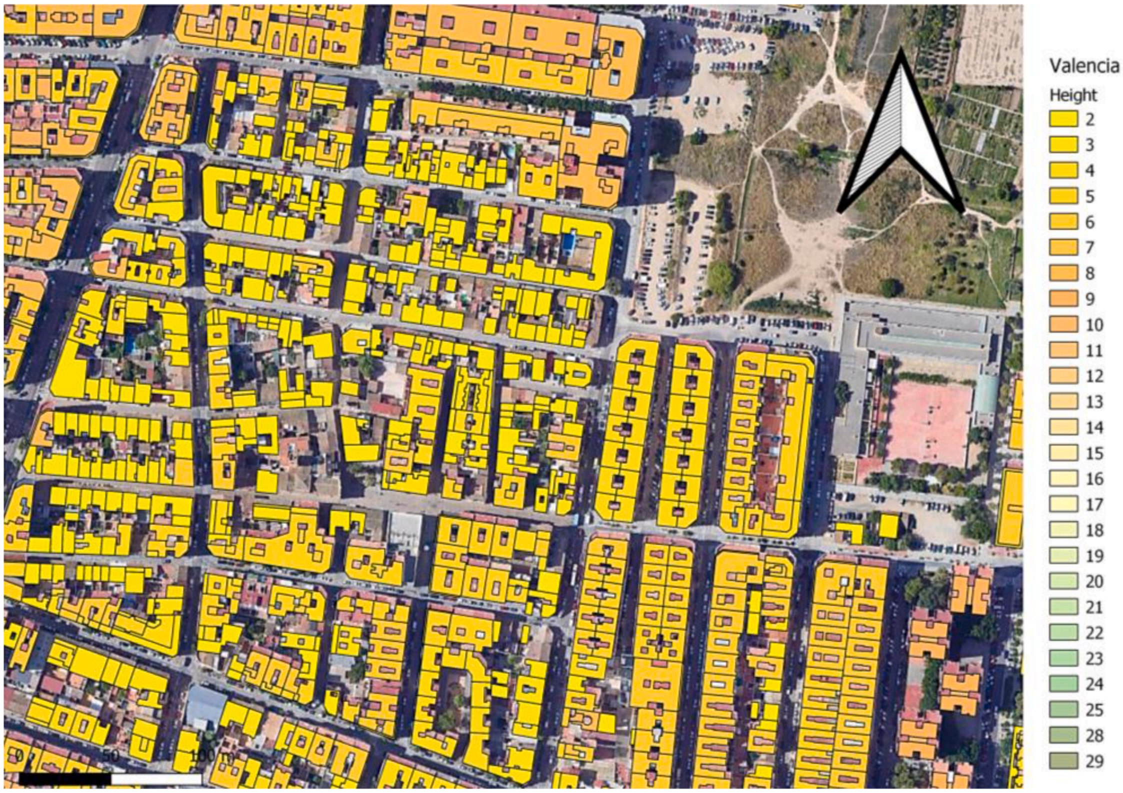

Fig. 2. Graphic illustration of the effects of filtering out spatial polygons of less than one height and less than 20 m^2 in the city of Valencia. Note the effect of the filter in the lower residential buildings in the center and the light shafts in higher buildings. Source: Own elaboration with QGIS.

Fig. 3. Graphic illustration of the effects of filtering out spatial polygons of less than one height and less than 20 m^2 in one municipality of the 2nd ring (San Antonio de Benagéber). Note the significant number of buildings discarded. Source: Own elaboration with QGIS.

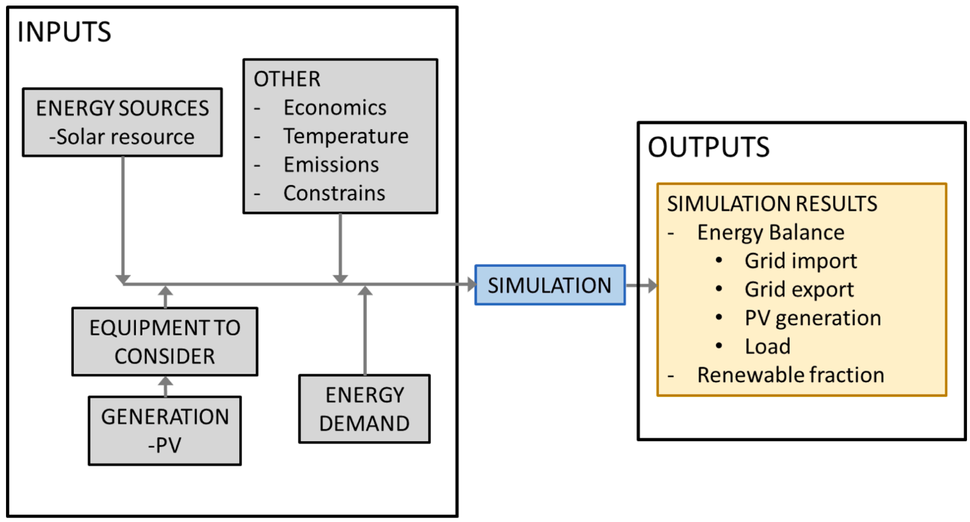

Fig. 4. Schematic overview used for developing this work - inputs and outputs of HOMER Software.

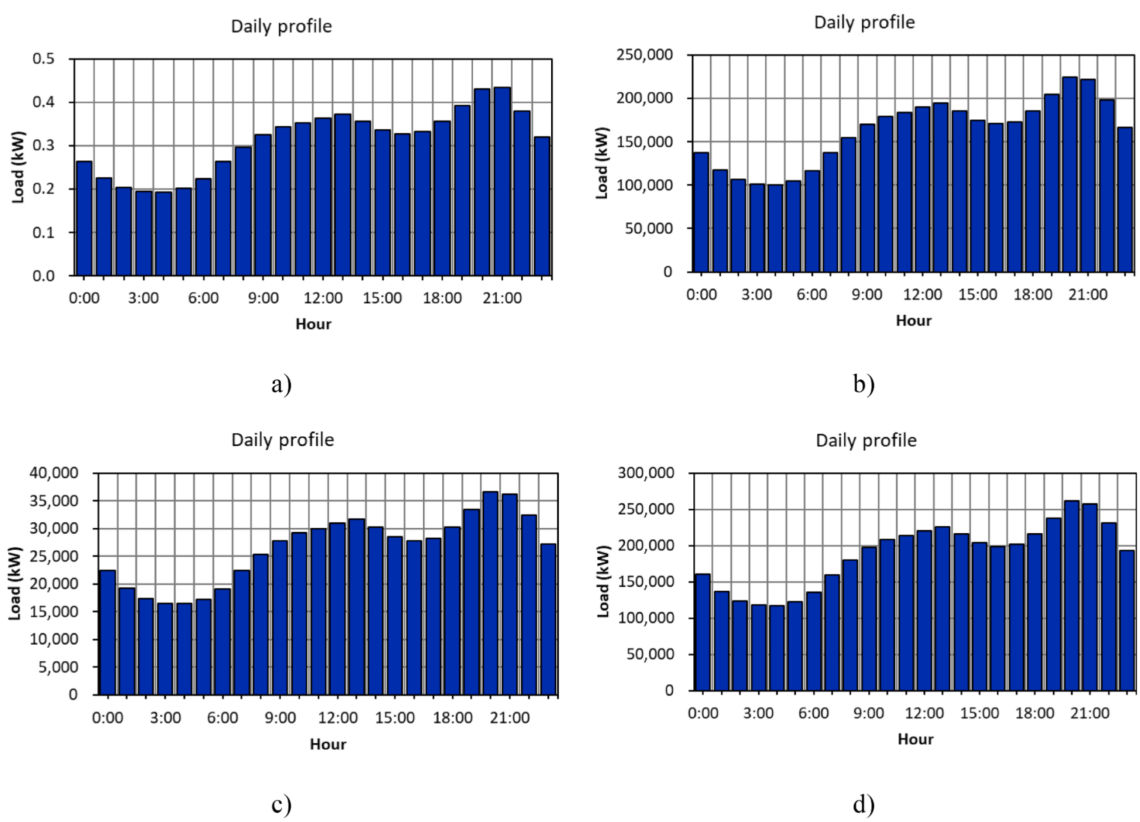

Fig. 5. Average energy demand: a) daily profile for one household b) daily profile first ring c) daily profile second ring. d) daily profile first + second ring. Source: adapted from (Dades estadístiques de la ciutat de València - València 2022), (Consulta los perfiles de consumo (TBD) | Red Eléctrica 2022), and (HOMER, 'HOMER Pro' 2022).

residential rooftops for PV production. As estimated from the residential polygons of more than one height in the cadastre database, the area of all the buildings is added up. The result is the available area in residential rooftops in each municipality, disaggregated by building height (from 2 to 9+ heights). This level of disaggregation is relevant, as electricity demand differs by building height. For each municipality, the number of buildings and households per height has been obtained from official data from Instituto Nacional de Estadística.

The actual rooftop area for PV exploitation is estimated by applying a factor of 50% to the residential rooftop area. This factor is in line with other estimates for Valencia and a review of relevant studies (Gómez-Navarro, Brazzini, Alfonso-Solar, and Vargas-Salgado, 2021).

2.4. Simulations

A scheme of required inputs and obtained outputs is shown in Fig. 4. The main inputs needed are solar resources, peak power to be installed (estimated employing QGIS) on the roof, and energy demand. On the other hand, produced energy and information about the economic analysis are obtained (LCOE, NPC, Payback, etc.)

Table 2
Total energy demand per kind of residential building (both rings)

Number of floors	kWh/year/ building	kWh/day/ building	GWh/year/all the buildings
2	3,735	10.2	174,8
3	7,079	19.4	84,2
4	23,380	64.1	121,1
5	32,764	89.8	230,0
6	41,646	114.1	302,1
7	54,391	149.0	154,2
8	60,884	166.8	363,8
9+	95,740	262.3	225,9
Total	18,538	50.8	1,656,1

2.4.1. Energy demand

The energy consumption is obtained from the statistical office of the Valencia council (Dades estadístiques de la ciutat de València - València 2022). This statistical data allows calculating the average annual electricity consumption per residential household and for the first and the second rings in Valencia. The resulting Fig. is 2,730 kWh/year. To obtain the hourly electricity demand profile (for the 8,760 values in one entire year), first, a typical curve for a Spanish household is obtained from the Spanish power system operator (Consulta los perfiles de consumo (TBD) | Red Eléctrica 2022). The curve is scaled using the 2,730 kWh/year previously calculated (Fig. 5). Finally, the total electricity demand profile is obtained by multiplying this profile by the total number of households.

To estimate the yearly energy demand the Eqs. (1) to (3) are used:

$$E_{1st\_ring\_y} = \sum_{i=1}^{i=8760} E_{1st\_ring\_h_i} = E_{house\_y} \cdot N_{1st_{ring}} \quad (1)$$

$$E_{2nd\_ring\_y} = \sum_{i=1}^{i=8760} E_{2nd\_ring\_h_i} = E_{house\_y} \cdot N_{2nd\_ring} \quad (2)$$

$$E_{1st\_ring+2nd\_ring\_y} = \sum_{i=1}^{i=8760} E_{1st\_ring+2nd\_ring\_h_i} = E_{house\_y} \cdot N_{1st\_ring+2nd\_ring} \quad (3)$$

The yearly profile of the Energy consumption per hour is obtained using the Eqs. (4) to (7):

$$E_{house\_h\_i} = C_i \cdot E_{house\_y} \quad (4)$$

$$E_{1st\_ring\_h\_i} = C_i \cdot E_{1st\_ring\_y} \quad (5)$$

$$E_{2nd\_ring\_h\_i} = C_i \cdot E_{2nd\_ring\_y} \quad (6)$$

$$E_{1st\_ring+2nd\_ring\_h\_i} = C_i \cdot E_{1st\_ring+2nd\_ring\_y} \quad (7)$$

Where

E_{house_y} is the energy consumption of an average house for one year. It is equal to 2,730 kWh/year

$E_{1st\_ring\_y}$ is the energy consumption of the first ring during one year

$E_{2nd\_ring\_y}$ is the energy consumption second ring during one year

$E_{1st+2nd\_ring\_y}$ is the energy consumption of the first and the second ring during one year

E_{h_i} is the energy consumed in the hour i

N_{1st_ring} is the number of households in the first ring, it is equal to 522,055

N_{2nd_ring} is the number of households in the second ring, it is equal to 85,245

$N_{1st\_ring+2nd\_ring}$ is the number of households in the first and second ring, it is equal to 607,300

i is the hour of the year. Its value goes from 1 to 8760.

C_i is the coefficient for every hour of the year. It represents the fraction of the annual consumption for each hour of the year. It is taken from ('Instituto Nacional de Estadística. (National Statistics Institute) 2022) (power system operator in Spain).

2.4.2. Estimation of Peak power

The peak power installed in the usable surface is an input for the simulation, used to obtain the energy produced by the PV system. The Peak Power is estimated by Eq. (8), obtained from (Gómez-Navarro, Brazzini, Alfonso-Solar, and Vargas-Salgado, 2021).

$$P_{Peak} = \frac{S_{Roof} \cdot F_S \cdot PV_{surf}}{1000} \quad (8)$$

Where:

P_{Peak} is the peak power of the PV system in kW.

S_{roof} is the surface available on the rooftop in m^2. This value is estimated from QGIS.

F_S is the surface factor (dimensionless value ranged from 0 to 1)

PV_{surf} is the peak power able to be installed on the useful rooftop surface in W/m^2

2.4.3. Electricity price

The power tariff has been estimated using the maximum value of demand power. The power rate is shown in Table 3

1.4.4. Solar resource

The global irradiation for the Valencia region is shown in Fig. 6; it represents a Typical Meteorological Year (TMY) (average hourly data for ten years). This information was taken from the PVGIS database (PVGIS 2022).

2.4.5. PV system components and cost

The PV panels were selected by comparing different alternatives available in the market. Due to the room limitations for setting up PV systems in an urban environment and its cost per kWp, panels with an efficiency bigger than 20% have been selected. To reduce the cost per kW$_p$ and increase efficiency, most PV panels use Passivated Emitter and Rear Cell (PERC) and half-cut technologies, being the peak power bigger than 350 W. The panel selected is the Vertex TSM-DE18M of 500 W. Its cost is 0.35 €/W VAT included. The PV panel datasheet is shown in Table 4.

The cost and type of the inverter depends on the size of the PV system and the kind of grid where the installation will be connected (single phase of three-phase). The inverter datasheet is shown in Table 5.

In European project ProSumE (ProSumE, 'ProSumE' 2022) it has been estimated the installation cost (It only includes labor cost) of companies dedicated to solar photovoltaic installations in Valencia (Fig. 7).

2.4.6. Other assumptions

The estimated photovoltaic system used derating factor is 0.9. The derating factor considers the soiling of the panels, wiring losses, shading, snow cover, aging, etc, so a derating factor of 0.9 indicates 10% losses. Since calculation losses due to temperature have been estimated by HOMER using hourly temperature data, this factor does not include such temperature-related losses. On the other hand, another assumption is the percentage of surface to be used to estimate the peak power able to be installed on the usable rooftop. To calculate the usable surface, this study follows the method used in (Gómez-Navarro, Brazzini, Alfonso-Solar, and Vargas-Salgado, 2021), which estimated that Valencia City could exploit 50% of the available rooftop surface ($F_s = 0,5$). Detailed information can be found in the report mentioned. Finally, taking into account PV panel dimensions and characteristics (in Table 4), optimal panel tilt (35° faced to the south according to PVGIS (PVGIS 2022) for Valencia), and applying the Winter Solstice classical trigonometric method (Castellano, Gázquez Parra, Valls-Guirado, and Manzano-Agugliaro, 2015), it was obtained the peak power able to be installed on the useful rooftop surface (PV_{surf}) is 100 W/m^2.

Table 3
Electricity, sellback, and average demand price for the three periods. Adapted from (Red Electrica ESIOS 2022) (From Jun 2021 to Feb 2022)

Rate	Electricity Price €/kWh	Sellback Rate €/kWh	Demand Rate €/kW/month	Applicable
P3 Off peak	0.197	0.153	0.12	Jan-Dec Weekdays 00:00-08:00 Jan-Dec Weekends 00:00-24:00
P2 Standard	0.247	0.168	2.78	Jan-Dec Weekdays 08:00-10:00, 14:00-18:00, 22:00-24:00
P1 Peak	0.287	0.175	2.78	Jan-Dec Weekdays 10:00-14:00, 18:00-22:00

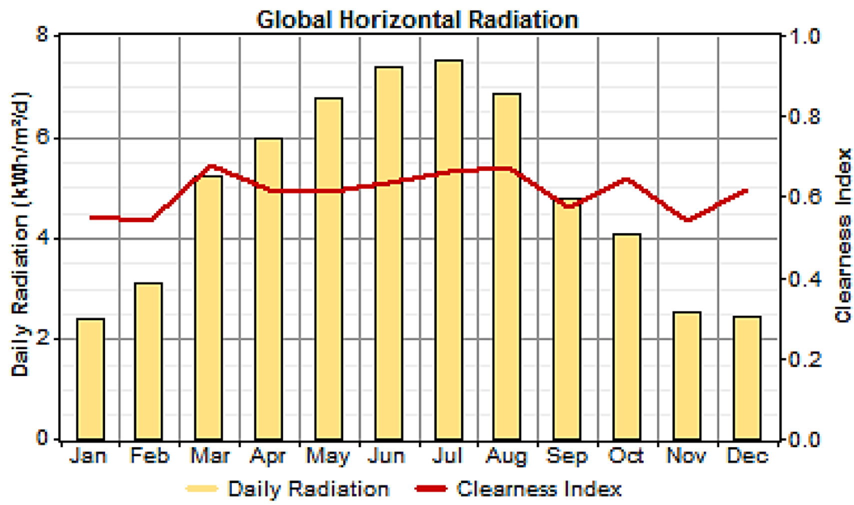

Fig. 6. Global Horizontal Radiation in kWh/m^2/day for every studied case. Source: Adapted from Homer ® with data from (PVGIS 2022).

Table 4
Datasheet of the selected PV panels for all the cases. Source: (TECHNOSUN 2022)

Parameter	Abbreviation	Value	Units
Peak Power	P_{peak}	500	W
MPP Voltage	V_{MPP}	42.8	V
MPP Current	I_{MPP}	11.69	A
OC Voltage	V_{OC}	51.7	V
SC Current	I_{SC}	12.28	A
Efficiency	η	20.7	%
Dimensions		2187 × 1102 × 35	mm
Area		2.41	m^2
Cost (VAT included)		172	€

Table 5
Datasheet of the selected grid-tied inverters for every case. Source: (TECHNOSUN 2022) and (SMA 2022).

Brand	SolaX	SMA	
Model	X1 Boost 4.2	STP25000TL	
Number of inverters	1	4	
INPUT (DC)			
Max. PV array power	5,200	45,000	W
Maximum DC Voltage	600	1,000	V
Maximum input Current	12*	33*	A
Maximum SC Current	12.8*	43*	A
MPPT voltage range	70-580	390-800	V
No MPPT/Max strings per MPPT	2/1	2/3	
OUTPUT AC			
Phases	1	3	
Nominal AC power	4,200	25000	VA
Euro efficiency	97	98.1	%
Cost	688	2,566	€

* per MPPT tracker

2.5. Energy balance

In the energy balance it is compared the addition of electricity produced by the PV system and the electricity going from the grid to load (as PV and Grid are all the employed electricity sources), with the addition of electricity consumption (Load) and exported electricity from the PV system to the grid. This energy balance is represented by Eq. 9 and similar balane are applied in previous research (Korkas, Baldi, Michailidis, and Kosmatopoulos, 2016), (Vargas-Salgado, Aparisi-Cerdá, Alfonso-Solar, and Gómez-Navarro, 2022), to describe the interactions inside a grid-connected photovoltaic-equipped microgrid.

$$E_{PV} + E_{Grid\_to\_load} = E_{Load} + E_{PV\_to\_grid} \quad (9)$$

Where:
E_{PV} is the photovoltaic electricity generation
$E_{Grid\_to\_load}$ is the electricity taken from the grid and going to load
E_{Load} is the electricity demand (coming from the grid or the PV system)
$E_{PV\_to\_grid}$ is the electricity going from the PV system to the grid (exported electricity)

On the other hand, no renewable fraction f_{ren} is estimated through Eq. 10, obtained from (HOMER, 'HOMER Pro' 2022).

$$f_{ren} = 1 - \frac{E_{nonren}}{E_{tot}} \quad (10)$$

Where:
E_{noren} is the energy produced by non-renewable sources
E_{tot} is the total energy production

3. Results

This section presents the results: rooftop area available for PV exploitation, potential PV power generation, photovoltaic system coverage, and gains from the addition of energy exchange with metropolitan rings. Results are presented according to two energy exchange scenarios between geographical units. Scenario 1 includes the city of

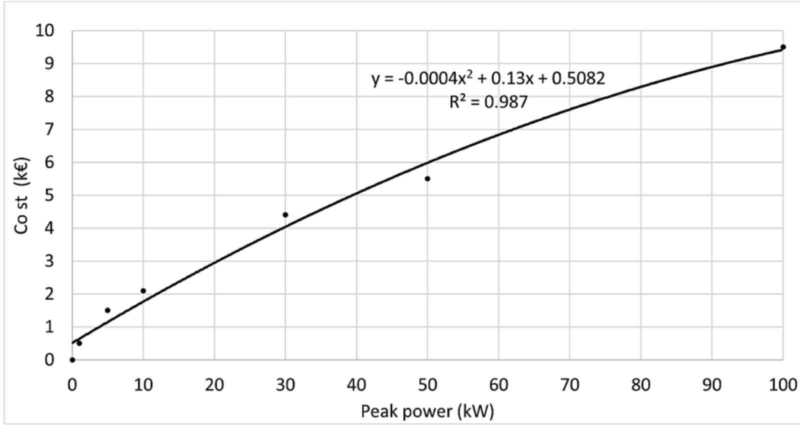

Fig. 7. PV system labor cost vs peak power. Adapted from (Vargas-Salgado, Aparisi-Cerdá, Alfonso-Solar, and Gómez-Navarro, 2022).

Valencia and the first ring of its metropolitan area (to be precise, the sample of municipalities accounting for about 70% of the population). Scenario 2 includes the city of Valencia and its metropolitan area's first and second.

The main result of the analysis is that the exchange of rooftop-mounted PV energy between the city of València and its metropolitan area (1st and 2nd ring) increases the coverage of residential load from 60.7% to 79.2%, or about 30% in relative terms, by adding 443.2 GWh/year of PV generation. The following sub-sections explain this result.

3.1. Rooftop area available for PV exploitation

Table 6 estimates the residential rooftop area available for PV exploitation. Based on publicly available cadastral data, the area has been estimated with the GIS software QGIS. To facilitate the comparison, Table 6 presents the estimation based on both available rooftop areas per building and household.

The rooftop area shows considerable variation between the first and second metropolitan ring, given, to a large extent, to the differences in the residential stock – higher buildings with more households in the first ring and lower buildings with fewer households in the second ring. As an illustration, the rooftop area per household in the 2nd ring is about 50% or more superior to the 1st ring.

3.1.1. Scenario 1: First metropolitan ring

Table 7 estimates the available rooftop area per building and household in Scenario 1 (exchange between València city and the 1^{st} metropolitan ring). Results show that, counterintuitively, available rooftop area per building increases with building height while, intuitively, rooftop area per household decreases.

Table 6
Rooftop area per household in the 1^{st} and 2^{nd} ring. Source: Adapted from cadastral and statistical data employing QGIS.

	1st ring	2nd ring	2nd vs 1st ring
Number of floors	Rooftop area per household (m^2)	Rooftop area per household (m^2)	Relative increase in 2nd ring (as % of 1st ring rea)
2	80.5	92.4	14.8%
3	52.3	62.1	18.7%
4	25.4	42.2	66.1%
5	21.0	30.9	47.1%
6	18.6	28.6	53.8%
7	15.1	22.3	47.7%
8	12.1	19.3	59.5%
9+	9.3	16.0	72.0%

Table 7
Available rooftop area per type of height of building in the 1^{st} ring. Source: Adapted from cadastral and INE data employing QGIS.

Number of floors	Total rooftop surface - S_{roof} (m^2)	Residential buildings	Households	Rooftop area per household (m^2)
2	2,311,704	17,087	28,730	80.5
3	785,669	4,405	15,020	52.3
4	812,174	3,650	32,030	25.4
5	1,523,745	6,120	72,585	21.0
6	1,938,430	6,893	104,465	18.6
7	821,289	2,737	54,260	15.1
8	1,608,658	5,939	132,535	12.1
9+	764,819	2,341	82,430	9.3
Total	10,566,488	49,172	522,055	

Table 8
Available rooftop area per type of height of building in the 2^{nd} ring. Source: Adapted from cadastral and INE data employing QGIS.

Number of floors	Total rooftop surface - S_{roof} (m^2)	Residential buildings	Households	Rooftop area per household (m^2)
2	3,271,388	29,733	35,390	92.4
3	985,106	7,491	15,860	62.1
4	522,358	1,531	12,390	42.2
5	362,750	899	11,745	30.9
6	179,950	359	6,285	28.6
7	50,875	98	2,285	22.3
8	16,703	36	865	19.3
9+	6,799	19	425	16.0
Total	5,395,929	40,166	85,245	

3.1.2. Scenario 2: Second metropolitan ring

Table 8 presents the estimation of available rooftop area per building and per household in Scenario 2 (exchange of energy between València city and the 2nd metropolitan ring). Again, obtained results show an increase in the available rooftop area per building with height and a decrease in the available area per household.

3.1.3. Comparison between Scenario 1 and Scenario 2

As expected, the higher availability of rooftop area per household in the 2nd metropolitan ring shows that the latter is better suited to rooftop PV than the 1st metropolitan ring. The available surface per household in the 2nd ring ranges from 14.8% to 72% higher than in the 1st metropolitan ring. Additionally, it is important to notice that in the 1st ring the percentage of buildings with 2 floors is only 21.9%; however, this percentage for the 2nd ring is 60.6%.

This effect helps to counterweigh the impact of the lower number of buildings – i.e., less potential installations – in the 2nd ring (49,172 vs 40,166 buildings in the 1st and 2nd ring, respectively, or 18.3% less buildings in the 2nd ring).

3.2. PV rooftop potential

This section presents the energy balance, estimating the rooftop PV potential in the 1st and 2nd rings under a grid-tied PV system scheme. Also, it presents an estimation of the rooftop PV potential for the ensemble of the metropolitan area (Valencia city and 1st and 2nd rings). Finally, information about the energy demand covered by the PV system is given.

3.2.1. Scenario 1: First metropolitan ring

Table 11 shows the calculation results for the 1st metropolitan ring (València city plus five sampled municipalities). As expected, the PV system's coverage varies considerably with the height of buildings. Buildings of lower height can potentially provide a higher percentage of the load. Table 4 shows the results of the analysis. Thus, buildings of 2 floors are estimated to be able to provide 82% of the load with PV systems and can export about 1.98 MWh per MWh of load, so they are net generators. The opposite occurs for buildings of 9 heights or more, for which PV systems can provide 28% of their load without exporting because all the generation is self-consumed.

To compare the obtained results, it contrasted obtained results for the city of Valencia with the estimation of rooftop available surface and PV generation in (Gómez-Navarro, Brazzini, Alfonso-Solar, and Vargas-Salgado, 2021). Once differences in methods are considered (the most relevant being the consideration of commercial and non-residential buildings in (Torres-Rivas, Palumbo, Jiménez, and Boer, 2022)), both estimates are of the same magnitude.

Table 10 presents the energy results for the 1st metropolitan ring. The PV coverage rate for the ensemble of the city of València and the 6 municipalities in the sample amounts to 60.9%. The estimates are obtained as follows: a) energy demand. from data and assumptions in Section 2.5; b) PV energy production, from the extrapolation of an average residential building as in Table 9; and PV coverage rate, as the ratio b/a.

3.2.2. Scenario 2: Second metropolitan ring

Table 11 shows the analysis of PV potential per the building height for the 2nd metropolitan ring (15 municipalities). Results show considerable improvement in the percentage of load that PV systems can cover. It is estimated that buildings of 2 floors in the 2nd ring can provide 84% of their energy demand with PV systems (and can export about 2.31 MWh per MWh of load), while, on the other end, the same figure for buildings of 9 heights amounts to 43% (with reduced exports, only 0.12 MWh per MWh of load).

Table 12 presents the energy results for the 2nd metropolitan ring. The PV coverage rate for the ensemble of the city of València and the 6 municipalities in the sample amounts to 190.7%. The estimates are obtained as follows: a) energy demand. from data and assumptions in Section 2.5; b) PV energy production, from the extrapolation of an average residential building as in Table 11; and PV coverage rate, as the ratio b/a.

A direct implication of Tables 10 and 12 is that it is also possible, from Scenarios 1 and 2, to estimate the PV coverage rate for the whole metropolitan area (Valencia, 1st ring and 2nd ring). Table 13 presents such figures. The PV coverage rate in Table 13 thus represents the percentage of electricity demand in the residential stock of the whole metropolitan area that PV generation can be expected to fulfill under the assumption of this study. The main result in Table 13 is an estimated PV coverage rate of 79.2% for the whole metropolitan area. This implies that the exchange of rooftop-mounted PV energy between the city of València and its metropolitan area (1st and 2nd ring) increases the coverage of residential load from 60.7% to 79.2%, or about 30% in relative terms, by adding 443.2 GWh/year of PV generation.(Fig. 8)

4. Discussion

This study has found that energy exchanges between the city of Valencia and its metropolitan ring could represent a potential increase in the PV coverage rate o from 60.9% (1st ring alone) to 79.2% (ensemble of 1st and 2nd ring) – or about 30% in relative terms. Additionally, the analysis per building with a different number of floors shows that, on average, for more than four floors potential PV generation is lower than the load, thus setting an upper limit for net self-sufficiency in Valencia.

At the same time, the authors are aware of significant limitations in their results. First and foremost, the study has been confined to the satisfaction of residential demand. This stems partly from

Table 10
Electrical demand coverage by the height of all the building in the 1st ring. Source: Adapted from HOMER results

Height of the building	Energy demand (GWh/year)	PV Energy production (GWh/year)	PV coverage rate
2	78.3	190.7	243.4%
3	41.0	64.3	157.1%
4	87.3	66.5	76.1%
5	197.9	124.6	62.9%
6	284.9	159.5	56.0%
7	148.0	67.4	45.5%
8	361.4	131.6	36.4%
9+	224.8	62.6	27.9%
Total	1,423.6	867.2	60.9%

Table 9
Energy balance for an average residential building, by the height of the building in the 1st ring. Source: Adapted from HOMER results.

Number of floors	2	3	4	5	6	7	8	9+
PV generation - E_{PV} (MWh)	11.2	14.6	18.2	20.4	23.2	24.6	22.2	26.8
From grid - $E_{Grid\_to\_load}$ (MWh)	2.5	5.1	14.2	19.7	25.6	34.7	41.0	69.6
Load - E_{Load} (MWh)	4.6	9.3	23.9	32.3	41.3	54.1	60.8	96.0
To grid $E_{PV\_to\_grid}$ (MWh)	9.0	10.4	8.5	7.7	7.4	5.3	2.4	0.4
Percentages								
PV generation - E_{PV}	81.9%	74.1%	56.2%	50.9%	47.5%	41.5%	35.1%	27.8%
From grid - $E_{Grid\_to\_load}$	18.1%	25.9%	43.8%	49.1%	52.5%	58.5%	64.9%	72.2%
Load - E_{Load}	33.7%	47.1%	73.8%	80.7%	84.7%	91.1%	96.2%	99.6%
To grid $E_{PV\_to\_grid}$	66.3%	52.9%	26.2%	19.3%	15.3%	8.9%	3.8%	0.4%
PV coverage rate	243.0%	157.1%	76.2%	63.0%	56.1%	45.6%	36.5%	27.9%
Renewable fraction	81.9%	74.1%	56.2%	50.9%	47.5%	41.5%	35.1%	27.8%

Table 11
Energy balance for an average residential building, by the height of the building in the 2nd ring. Source: Adapted from HOMER results.

Number of floors	2	3	4	5	6	7	8	9+
PV generation - E_{PV} (MWh)	9.0	10.9	28.1	33.2	41.3	42.7	38.1	29.4
From grid - $E_{Grid\_to\_load}$ (MWh)	1.7	3.1	12.4	20.6	27.9	38.3	40.4	38.8
Load - E_{Load} (MWh)	3.3	5.8	22.1	35.6	47.7	63.6	65.5	61.0
To grid $E_{PV\_to\_grid}$ (MWh)	7.5	4.3	16.8	18.2	21.4	17.5	13.0	7.2
Percentages								
PV generation - E_{PV}	83.9%	77.6%	69.4%	61.7%	59.7%	52.7%	48.6%	43.1%
From grid - $E_{Grid\_to\_load}$	16.1%	22.4%	30.6%	38.3%	40.3%	47.3%	51.4%	56.9%
Load - E_{Load}	30.2%	57.4%	56.9%	66.2%	69.1%	78.4%	83.5%	89.5%
To grid $E_{PV\_to\_grid}$	69.8%	42.6%	43.1%	33.8%	30.9%	21.6%	16.5%	10.5%
PV coverage rate	278.2%	188.0%	127.3%	93.2%	86.4%	67.2%	58.2%	48.2%
Renewable fraction	83.9%	77.6%	69.4%	61.7%	59.7%	52.7%	48.6%	43.1%

Table 12
Electrical demand coverage by the height of the building in the 2nd ring. Source: Adapted from HOMER results

Height of the building	Energy demand (GWh/year)	PV Energy production (GWh/year)	PV coverage rate
2	96.5	268.4	278.1%
3	43.3	81.1	187.6%
4	33.8	43.0	127.2%
5	32.0	29.8	93.1%
6	17.1	14.8	86.3%
7	6.2	4.2	67.1%
8	2.4	1.4	58.1%
9+	1.2	0.6	48.2%
Total	232.5	443.2	190.7%

Table 13
Electrical demand coverage by the height of the building in the 1nd +2nd ring. Source: Adapted from HOMER results

Height of the building	Energy demand (GWh/year)	PV Energy production (GWh/year)	PV coverage rate
2	174.9	461.1	263.7%
3	84.2	144.5	171.6%
4	121.1	109.7	90.6%
5	230.0	154.4	67.1%
6	302.0	173.8	57.5%
7	154.2	71.7	46.5%
8	363.8	133.4	36.7%
9+	225.9	63.1	27.9%
Total	1,656.1	1,311.5	79.2%

methodological considerations – i.e., the difficulties associated with estimating industrial electricity hourly demand in large geographical units such as metropolitan areas – but also from the explorative nature of the performed analysis. A second key limitation concerns the omissions and incorrection in the datasets. Throughout the analysis, important errors were detected in the cadastral database, e.g. height of spatial polygons. To address this issue, the methodology has been consistent in its choices in the direction of underestimating the PV potential. The overall result is a conservative estimate of the PV coverage rate. A third limitation is that residential electricity consumption has been estimated with present figures, without consideration of its possible evolution in the next decades in parallel to the deployment of rooftop PV. As it is self-evident, this assumption has a significant effect in estimating the percentage of demand PV can potentially cover. Lastly, the analysis is limited to the satisfaction of electricity demand with solar PV, thus leaving aside non-electrical energy consumption in households. As the electrification of European economies is likely to make progress in the next decades, the results of this study will become more relevant. At this point, it is very adventurous to estimate whether or not the foreseeable electrification of European economies will counterweight the reductions in demand due to higher efficiency and more austere habits. In either case, the calculations will need to be adjusted accordingly.

5. Conclusion

This study set out to quantify how much PV rooftops in metropolitan areas can contribute to addressing the 'wicked' problem of energy self-sufficiency in dense, compact Mediterranean cities. The question has been explored in a case study, the city of Valencia and its metropolitan area, and more specifically, in the less-favorable case of the coverage rate of the residential stock. The study has compared the PV potential of the city and its first ring of metropolitan municipalities with the 2nd outer ring and the 1st and 2nd ring ensemble. Results show a significant potential for the PV coverage rate of the electric demand of the residential stock.

Future methodological improvements may include a higher degree of

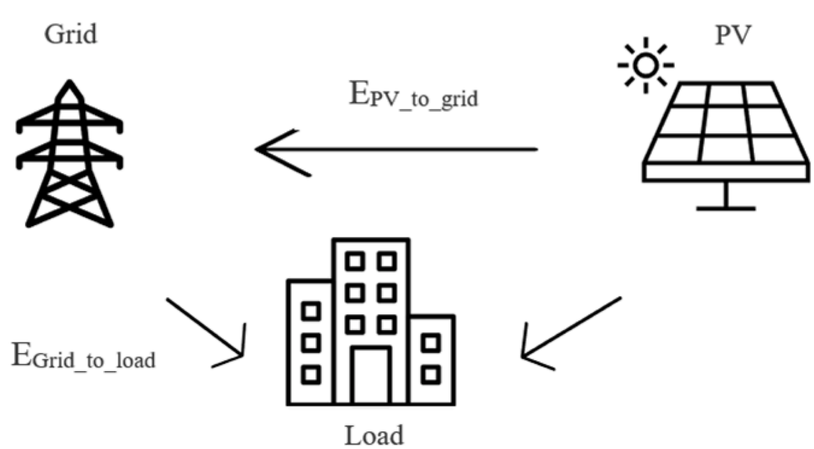

Fig. 8. Energy balance carried out in the simulations.

automation in estimating the exploitable rooftop surface for the sake of replicability and scalability. Another development line would include introducing shared consumption and energy community models, testing alternative datasets, and extending the analysis beyond the residential domain. A more comprehensive model would also include the full range of categories of electricity consumption and the full range of electricity sources available in metropolitan areas. Last but not least, exceeding the techno-economic analysis and progressing towards assessing the market uptake of the PV solutions hypothesized in this study would yield more relevant results for energy planning and policymaking in general. Other schemes generator-consumer, such as P2P must be analysed to improve the study.

Results of the methodology applied to the Valencia metropolitan area suggest that European cities would do well to expand their planning beyond their administrative boundaries. This may hold especially true for dense, compact Mediterranean cities, where the availability of rooftop space for PV generation is limited. In this case, city planners could reflect upon how to introduce metropolitan energy planning in their planning programs, notably the Sustainable Energy and Climate Action Plans (SECAP). More broadly, should dense, compact Mediterranean cities fail to achieve 100% energy autarky in the coming decades, as it seems likely, this must not necessarily translate into an imperative to 'colonize' rural areas with utility-scale ground-mounted PV plants. Cities may also seek complementary strategies, such as curtailing electricity demand as well as resorting to small- and medium-scale PV generation in anthropized, barren tracts of land, hopefully thus avoiding greater evils.

Declaration of Competing Interest

The authors declare that they have no known competing financial interests or personal relationships that could have appeared to influence the work reported in this paper.

Data availability

The authors do not have permission to share data.

Acknowledgements

This work has been supported by: Modelado, experimentación y desarrollo de sistemas de gestión óptima para microrredes híbridas renovables (CIGE/2021/172). (01/01/22 - 31/12/23). Investigación competitiva proyectos. GENERALITAT VALENCIANA.

Renewable Energies System For Cities RES4CITY (101075582). (01/10/22 - 30/09/25). HORIZON-CSA, EUROPEAN COMMISSION.

Chair of Urban Energy Transition, UPV - Las Naves and Fundació València Clima i Energia, Ajuntament de València, Spain.

Supplementary materials

Supplementary material associated with this article can be found, in the online version, at doi:10.1016/j.scs.2023.104727.

References

Aparisi-Cerdá, I., Ribó-Pérez, D., Cuesta-Fernandez, I., & Gómez-Navarro, T. (2022). Planning positive energy districts in urban water fronts: Approach to La Marina de València, Spain. *Energy Conversation and Management, 265*, Article 115795.

Bergamasco, L., & Asinari, P. (2011). Scalable methodology for the photovoltaic solar energy potential assessment based on available roof surface area: Further improvements by ortho-image analysis and application to Turin (Italy). *Solar Energy, 85*(11), 2741–2756. https://doi.org/10.1016/j.solener.2011.08.010

Burger, S. P., & Luke, M. (2017). Business models for distributed energy resources: A review and empirical analysis. *Energy Policy, 109*, 230–248. https://doi.org/10.1016/j.enpol.2017.07.007

Bódis, K., Kougias, I., Jäger-Waldau, A., Taylor, N., & Szabó, S. (2019). A high-resolution geospatial assessment of the rooftop solar photovoltaic potential in the European Union. *Renewable and Sustainable Energy Reviews, 114*, Article 109309. https://doi.org/10.1016/j.rser.2019.109309

Capellán-Pérez, I., Campos-Celador, Á., & Terés-Zubiaga, J. (2018). Renewable energy cooperatives as an instrument towards the energy transition in Spain. *Energy Policy, 123*, 215–229. https://doi.org/10.1016/j.enpol.2018.08.064

Castellano, N. N., Gázquez Parra, J. A., Valls-Guirado, J., & Manzano-Agugliaro, F. (2015). Optimal displacement of photovoltaic array\'s rows using a novel shading model. *Applied Energy, 144*, 1–9. https://doi.org/10.1016/j.apenergy.2015.01.060

Castellanos, S., Sunter, D. A., & Kammen, D. M. (2017). Rooftop solar photovoltaic potential in cities: how scalable are assessment approaches? *Environmental Research Letters, 12*(12), Article 125005. https://doi.org/10.1088/1748-9326/aa7857

Choi, Y., Suh, J., & Kim, S.-M. (2019). GIS-based solar radiation mapping, site evaluation, and potential assessment: A review. *Applied Sciences, 9*(9). https://doi.org/10.3390/app9091960. Art. no. 9.

'Consulta los perfiles de consumo (TBD) | Red Eléctrica'. https://www.ree.es/es/clientes/generador/gestion-medidas-electricas/consulta-perfiles-de-consumo (accessed Oct. 05, 2022).

Cramer, W., et al. (2018). Climate change and interconnected risks to sustainable development in the Mediterranean. *Nature Climate Change, 8*(11). https://doi.org/10.1038/s41558-018-0299-2. Art. no. 11.

'Dades estadístiques de la ciutat de València - València'. https://www.valencia.es/es/cas/estadistica/inicio (accessed Oct. 05, 2022).

Droege, P. (2018). *Urban Energy Transition: Renewable Strategies for Cities and Regions*. Amsterdam, Oxford and Cambridge, MA: Elsevier.

Eslami, H., Najem, S., Ghanem, D. A., & Ahmad, A. (2021). The potential of urban distributed solar energy in transition economies: The case of Beirut city. *Journal of Environmental Management, 285*, Article 112121. https://doi.org/10.1016/j.jenvman.2021.112121

Fakhraian, E., Forment, M. A., Dalmau, F. V., Nameni, A., & Guerrero, M. J. C. (2021). Determination of the urban rooftop photovoltaic potential: A state of the art. *Energy Rep, 7*, 176–185. https://doi.org/10.1016/j.egyr.2021.06.031

Fakhraian, E., Alier, M., Valls Dalmau, F., Nameni, A., & Casañ Guerrero, M. J. (2021). The urban rooftop photovoltaic potential determination. *Sustainability, 13*(13). https://doi.org/10.3390/su13137447. Art. no. 13.

Freitas, S., Catita, C., Redweik, P., & Brito, M. C. (2015). Modelling solar potential in the urban environment: State-of-the-art review. *Renewable and Sustainable Energy Reviews, 41*, 915–931. https://doi.org/10.1016/j.rser.2014.08.060

Fuster-Palop, E., Prades-Gil, C., Masip, X., Viana-Fons, J. D., & Payá, J. (2021). Innovative regression-based methodology to assess the techno-economic performance of photovoltaic installations in urban areas. *Renewable and Sustainable Energy Reviews, 149*, Article 111357. https://doi.org/10.1016/j.rser.2021.111357

P. Gagnon, R. Margolis, J. Melius, C. Phillips, and R. Elmore, 'Rooftop Solar Photovoltaic Technical Potential in the United States. A Detailed Assessment', NREL/TP–6A20-65298, 1236153, Jan. 2016. 10.2172/1236153.

Gassar, A. A. A., & Cha, S. H. (2021). Review of geographic information systems-based rooftop solar photovoltaic potential estimation approaches at urban scales. *Applied Energy, 291*, Article 116817. https://doi.org/10.1016/j.apenergy.2021.116817

Generalitat Valenciana, 'Pla Mobilitat Metropolità València'. [Online]. Available: https://www.pmomevalencia.com.

Groppi, D., de Santoli, L., Cumo, F., & Astiaso Garcia, D. (2018). A GIS-based model to assess buildings energy consumption and usable solar energy potential in urban areas. *Sustainable Cities and Society, 40*, 546–558. https://doi.org/10.1016/j.scs.2018.05.005

Gómez-Navarro, T., Brazzini, T., Alfonso-Solar, D., & Vargas-Salgado, C. (2021). Analysis of the potential for PV rooftop prosumer production: Technical, economic and environmental assessment for the city of Valencia (Spain). *Renewable Energy, 174*, 372–381. https://doi.org/10.1016/j.renene.2021.04.049

HOMER, 'HOMER Pro'. Dec. 16, 2022. [Online]. Available: https://www.homerenergy.com/products/pro/index.html.

Horváth, M., Kassai-Szoó, D., & Csoknyai, T. (2016). Solar energy potential of roofs on urban level based on building typology. *Energy Building, 111*, 278–289. https://doi.org/10.1016/j.enbuild.2015.11.031

Hosseini, S. E. (2019). Development of solar energy towards solar city Utopia. *Energy Sources, Part A: Recovery, Utilization and Environmental Effects, 41*(23), 2868–2881. https://doi.org/10.1080/15567036.2019.1576803

'Instituto Nacional de Estadística. (National Statistics Institute)'. https://www.ine.es/dynt3/inebase/index.htm?type=pcaxis&path=/t20/e244/edificios/p03/&file=pcaxis&L=0 (accessed Oct. 05, 2022).

Izquierdo, S., Rodrigues, M., & Fueyo, N. (2008). A method for estimating the geographical distribution of the available roof surface area for large-scale photovoltaic energy-potential evaluations. *Solar Energy, 82*(10), 929–939. https://doi.org/10.1016/j.solener.2008.03.007

Korkas, C. D., Baldi, S., & Kosmatopoulos, E. B. (2018). 9 - grid-connected microgrids: Demand management via distributed control and human-in-the-loop optimization. In I. Yahyaoui (Ed.), *Advances in Renewable Energies and Power Technologies* (pp. 315–344). Elsevier. https://doi.org/10.1016/B978-0-12-813185-5.00025-5.

Korkas, C. D., Baldi, S., Michailidis, I., & Kosmatopoulos, E. B. (2015). Intelligent energy and thermal comfort management in grid-connected microgrids with heterogeneous occupancy schedule. *Applied Energy, 149*, 194–203. https://doi.org/10.1016/j.apenergy.2015.01.145

Korkas, C. D., Baldi, S., Michailidis, I., & Kosmatopoulos, E. B. (2016). Occupancy-based demand response and thermal comfort optimization in microgrids with renewable energy sources and energy storage. *Applied Energy, 163*, 93–104. https://doi.org/10.1016/j.apenergy.2015.10.140

Lambarki, R., Maanan, M., & Rhinane, H. (2020). The evaluation of the photovoltaic potential in the urban environment Case of the Nador City /Morocco. In *Proceedings of the 2020 IEEE International conference of Moroccan Geomatics (Morgeo)* (pp. 1–6). https://doi.org/10.1109/Morgeo49228.2020.9121911

Margolis, R., Gagnon, P., Melius, J., Phillips, C., & Elmore, R. (2017). Using GIS-based methods and lidar data to estimate rooftop solar technical potential in US cities. *Environmental Research Letters, 12*(7), Article 074013. https://doi.org/10.1088/1748-9326/aa7225

Mi, Z., et al. (2019). Cities: The core of climate change mitigation. *Journal of Cleaner Production, 207*, 582–589. https://doi.org/10.1016/j.jclepro.2018.10.034

Morganti, M., Salvati, A., Coch, H., & Cecere, C. (2017). Urban morphology indicators for solar energy analysis. *Energy Procedia, 134*, 807–814. https://doi.org/10.1016/j.egypro.2017.09.533

Moura, R., & Brito, M. C. (2019). Prosumer aggregation policies, country experience and business models. *Energy Policy, 132*, 820–830. https://doi.org/10.1016/j.enpol.2019.06.053

Munoz, F. (2003). Lock living: Urban sprawl in Mediterranean cities. *Cities, 20*(6), 381–385. https://doi.org/10.1016/j.cities.2003.08.003

Natanian, J., & Auer, T. (2018). Balancing urban density, energy performance and environmental quality in the Mediterranean: A typological evaluation based on photovoltaic potential. *Energy Procedia, 152*, 1103–1108. https://doi.org/10.1016/j.egypro.2018.09.133

Natanian, J., Aleksandrowicz, O., & Auer, T. (2019). A parametric approach to optimizing urban form, energy balance and environmental quality: The case of Mediterranean districts. *Applied Energy, 254*, Article 113637. https://doi.org/10.1016/j.apenergy.2019.113637

PVGIS Photovoltaic Geographical Information System. https://joint-research-centre.ec.europa.eu/pvgis-photovoltaic-geographical-information-system_en (accessed Dec. 15, 2022).

Pincetl, S. (2017). Cities in the age of the Anthropocene: Climate change agents and the potential for mitigation. *Anthropocene, 20*, 74–82. https://doi.org/10.1016/j.ancene.2017.08.001

ProSumE, 'ProSumE', Dec. 2022. [Online]. Available: https://www.lasnaves.com/proyectos/prosume/?lang=es.

Ramirez Camargo, L., & Stoeglehner, G. (2018). Spatiotemporal modelling for integrated spatial and energy planning. *Energy, Sustainability and Society, 8*(1), 32. https://doi.org/10.1186/s13705-018-0174-z

Red Electrica ESIOS, 'SELF-CONSUMPTION SURPLUS ENERGY PRICE FOR THE SIMPLIFIED COMPENSATION MECHANISM', Dec. 2022. [Online]. Available: https://www.esios.ree.es/en/analysis/1739?vis=1&start_date=31-12-2020T00%3A00&end_date=30-12-2021T23%3A00&compare_start_date=30-12-2020T00%3A00&groupby=hour&compare_indicators=1014,1001.

Ren, H., Xu, C., Ma, Z., & Sun, Y. (2022). A novel 3D-geographic information system and deep learning integrated approach for high-accuracy building rooftop solar energy potential characterization of high-density cities. *Applied Energy, 306*, Article 117985. https://doi.org/10.1016/j.apenergy.2021.117985

Ruiz-Campillo, X., Gil, O., & García Fernández, C. (2022). Ready for climate change? An assessment of measures adopted by 45 mediterranean coastal cities to face climate change. In W. Leal Filho, & E. Manolas (Eds.), *Climate Change in the Mediterranean and Middle Eastern Region* (pp. 269–291). Cham: Springer International Publishing. https://doi.org/10.1007/978-3-030-78566-6_13. Eds.,Climate Change Management.

SMA, 'SUNNY TRIPOWER 15000TL /20000TL / 25000TL', Dec. 2022. [Online]. Available: https://b2b.technosun.com/web/image/132717?unique=0c94e96e0a93de4c1ebe81ad90e40fabbc71dab5.

Song, X., et al. (2018). An approach for estimating solar photovoltaic potential based on rooftop retrieval from remote sensing images. *Energies, 11*(11). https://doi.org/10.3390/en11113172. Art. no. 11.

TECHNOSUN, 'The Vertex Backsheet Monocrystalline Module'. Accessed: Dec. 16, 2022. [Online]. Available: https://b2b.technosun.com/web/image/537883?unique=a504372b487a82b6a4e1d8e0051551a40db9a80c.

TECHNOSUN, 'NEW FROM SOLAX X1-BOOST G3'. Accessed: Dec. 16, 2022. [Online]. Available: https://b2b.technosun.com/web/image/371915?unique=74a2ae9e3c573b65b78c517c2fe7caef55f3e060.

Torres-Rivas, A., Palumbo, M., Jiménez, L., & Boer, D. (2022). Self-consumption possibilities by rooftop PV and building retrofit requirements for a regional building stock: The case of Catalonia. *Solar Energy, 238*, 150–161. https://doi.org/10.1016/j.solener.2022.04.036

Vargas-Salgado, C., Aparisi-Cerdá, I., Alfonso-Solar, D., & Gómez-Navarro, T. (2022). 'Can photovoltaic systems be profitable in urban areas? Analysis of regulation scenarios for four cases in Valencia city (Spain). *Solar Energy, 233*, 461–477. https://doi.org/10.1016/j.solener.2022.01.057

Vartholomaios, A. (2017). A parametric sensitivity analysis of the influence of urban form on domestic energy consumption for heating and cooling in a Mediterranean city. *Sustainable Cities and Society, 28*, 135–145. https://doi.org/10.1016/j.scs.2016.09.006

Vulkan, A., Kloog, I., Dorman, M., & Erell, E. (2018). Modeling the potential for PV installation in residential buildings in dense urban areas. *Energy Building, 169*, 97–109. https://doi.org/10.1016/j.enbuild.2018.03.052

Yildirim, D., Büyüksalih, G., & Şahin, A. D. (2021). Rooftop photovoltaic potential in Istanbul: Calculations based on LiDAR data, measurements and verifications. *Applied Energy, 304*, Article 117743. https://doi.org/10.1016/j.apenergy.2021.117743